Ninth Symposium on Integrated Observing and Assimilation Systems for the Atmosphere, Oceans, and Land Surface (IOAS-AOLS)

3.4 APPLICATION OF GPS SLANT WATER VAPOR TOMOGRAPHY TO AN IHOP STORM CASE WITH SIMPLE CONSTRAINTS

Yuanfu Xie[1], J. Braun[2], A. E. MacDonald[1], and R. Ware[2]

[1] NOAA Research-Forecast Systems Laboratory, Boulder, CO [2] GPS Research Group /UCAR, Boulder, CO

1. INTRODUCTION

Due to atmospheric water vapor refractivity, microwave signals transmitting from the global positioning system (GPS) satellites are further delayed after they propagate through the atmosphere and are received by GPS receivers on the ground. These delays are integrations of the refractivity along GPS slant paths between satellites and receivers. Since refractivity is a function of water vapor (Bevis et al, 1994), a slant water vapor delay is defined as a function of integrated water vapor along a path. Braun et al., (2001, 2003) developed a scheme converting slant water vapor delays into integrated slant water vapor (SW) along these GPS paths under certain assumptions. They found that there are 0.15-0.23 mm errors due to various error sources in SW with magnitudes of 5mm, for examples, double-difference for eliminating clock errors, multi-path caused by ground reflection for low elevation angles, and antenna phase errors. The lowest elevation angle discussed in their validation is 10 degree. Such accurate slant water vapor data should result an accurate water vapor distribution through a tomography analysis combining with some other data sources based upon an OSSE by MacDonald et al. (2002). Through similar OSSEs, MacDonald and Xie (2003) also showed that a GPS receiver network with 100 km density could provide reasonable water vapor analysis for mesoscale water vapor prediction. However, there has not been any real data GPS tomography experiement comfirming the OSSE results if accurate SW is provided.

The International H2O Project (IHOP) 2002 is a field experiment over the Southern Great Plains (SGP) of the United States focusing on distribution of water vapor and its application to improving the understanding and prediction of convection. The region was an optimal location due to existing experimental and operational facilities, strong variability in moisture, and active convection. The IHOP region is shown in Fig. 1.

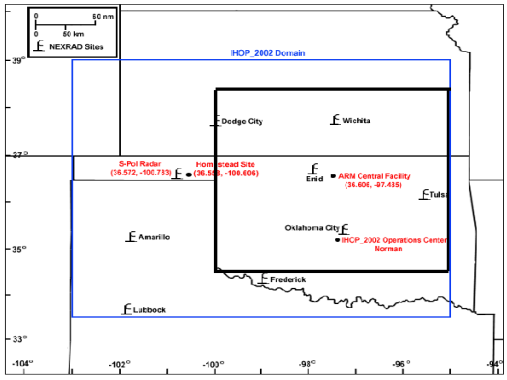

Fig. 1. *IHOP region is shown in the bigger rectangle frame. Our GPS analysis domain is marked by a thicker rectangluar frame over the right central IHOP domain.*

There are numbers of GPS receivers operating over NOAA/FSL stations, SuomiNet stations, and special stations deployed by CNRS CNRM/GAME France. In the right center of the IHOP region with left corner at latitude and longitude (34.5, -100.0) and right corner at (38.5, -95.0) as marked by a thicker frame, there are 25 receivers covering this 500 km by 500 km area. The locations of these 25 GPS receivers are plotted in Fig. 2. This GPS network has a roughly 100 km density close to the density requirement discussed by MacDonald and Xie (2003) and provides a reasonable

real time GPS tomography experiment environment.

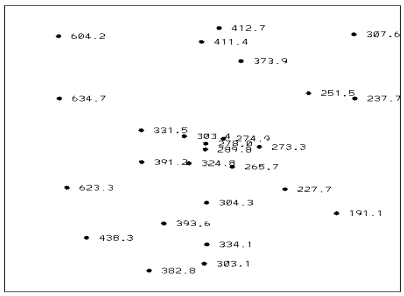

Fig. 2. *The 25 GPS locations in our GPS analysis domain.*

A GPS tomography analysis under this environment could provide us some confidence on the quality of the GPS slant water vapor data as well as the GPS slant tomography theory. We choose a storm case during June 12-13, 2002 and compare our analyses with the actual GOES satellite images and sounding data. The analysis basically reflects the water vapor distribution during the storm, and thus is a real GPS data case to confirm the OSSE results and the accuracy of SW for this storm case. More real GPS cases will be analyzed in the future.

The GPS tomography technique used in the analysis will be described in the next section; a discussion is presented in Section 3 on solution multiplicity of a ground-based GPS tomography analysis and some simple constraints for restricting the multiplicity. Real-time GPS water vapor tomography analyses will be demonstrated in Section 4. Final comments will be presented in Section 5.

2. GPS TOMOGRAPHY

GPS tomography is a direct analysis of observed GPS slant water vapor for deriving a three-dimensional water vapor distribution, independent of observations of other atmospheric elements and numerical models as needed for other variational analysis. MacDonald et al., (2002) presented their GPS tomography in detail using grid controls combined with a multigrid technique in retrieving water vapor distribution over resolvable scales from GPS slants. Here a different method is tested as an alternative of multigrid to solve the tomography problem. A recursive filter (Hayden and Purser, 1995) is applied to the control grid in order to replace the multigrid technique. Its smoothing parameter is used to directly control its analysis scales. A filter is applied to x, y and z directions one after another to achieve three-dimensional filter effect. Assuming this three-dimensional filter to be F, define a variable w such that

$$q = Fw,$$

where q is the water vapor grid function to be solved. Using the grid function q to calculate the Riemann sum (MacDonald et al., 2002) along a given GPS path between a satellite and a receiver, a GPS tomography cost function can be formed by summing the squares of the differences between observed GPS slants of water vapor and the corresponding Riemann sums which approximate the integrals of the water vapor. By choosing a proper recursive filter smooth parameter, irresolvable small-scale water vapor distribution is eliminated from the analysis so that the multigrid technique can be skipped. We choose the recursive filter scale parameter $\alpha = 0.7$ for the horizontal filters and 0.5 for the vertical filter with 21 grid-points in each direction. The reason of having a smaller scale parameter in the vertical direction is that water vapor has significant vertical variation, as its magnitude decays exponentially as height increases. The cost function can be viewed as a function of w through q and whenever q is needed, applying F to w to yield this grid function.

A disadvantage of the filter approach is that some simple known bounds of water vapor cannot be directly applied, for example, $q \geq 0$ in addition to the empirical selection of a scale parameter. For GPS water vapor tomography, this simple bound not only makes the analysis physically meaningful, but helps to reduce solution multiplicity shown in the next section. For the first pass of the recursive filter,

$$q_1 = (1-\alpha)w_1$$
$$q_i = \alpha q_{i-1} + (1-\alpha)w_i,$$

it is sufficient for $q \geq 0$ if $w \geq 0$. This bound of $w \geq 0$ is applied in the minimization problem.

To solve the tomography problem with a bound of $w \geq 0$, a limited BFGS for simple bound minimization algorithm (Byrd et al., 1995) is used. The gradient of the cost function is computed by an adjoint code generated by the TAMC software (Giering and Kaminski, 1998). The adjoint code is carefully tested using finite difference approximation of the gradient.

3. SIMPLE CONSTRAINTS

No matter how many ground based GPS slants water vapor integrals are available, they cannot uniquely determine a three-dimensional water vapor field. A simple example to illustrate this problem is the following. Considering a constant water vapor field in an x and z plane (assuming a water vapor field is not a function of y in a three-dimensional water vapor tomography), and a linear decreasing water vapor field in height in the same plane as shown in the following diagrams.

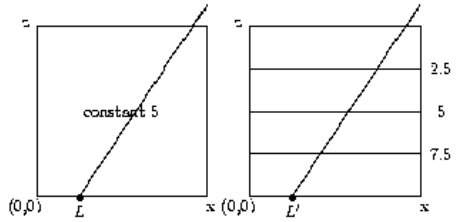

Along the lines, L and L', integrations of these water vapor fields will be the same as long as the slant goes through the top not the sides, i.e., they cannot show the difference of the two fields at all. GPS slant water vapor is called incomplete observations of water vapor. To determine water vapor distribution over certain scales, other information sources have to be introduced, physical constraints or direct water vapor observations. A more complex example is to add a field δq in the x and z plane shown in Fig. 3 to any given water vapor field in the same x and z plane.

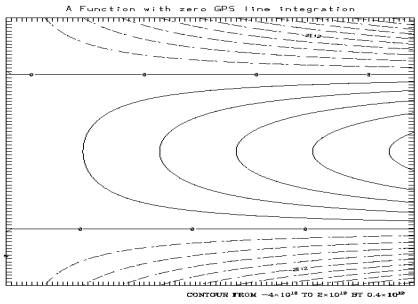

Fig. 3. *A δq field. Any GPS slant passing through the top of our domain cannot tell this difference between two water vapor distributions.*

Line integrals of $q+\delta q$ and q along any GPS path which passes through the top of the domain will be the same. Actually, we can construct more complex examples. In general, the smaller scales the analysis is to retrieve, the more freedom to determine a solution. In other words, the large-scale water vapor distribution requires less other data sources or constraints.

MacDonald et al. (2002) combined surface data and microwave profiler data into a GPS tomography problem as additional vertical water vapor information to eliminate the tomography multi-solutions problem for the scales of interest. Introducing surface and profiler observations, MacDonald et al. (2002) added the squares of the differences between interpolated water vapor from its grid values and the actual observations into the cost function as penalty terms. Since the majority of water vapor stays near the ground, or say below 5 km in height, accurate surface data and profiler data help eliminate the other solutions fitting the GPS slants. This method seems to be working well if there are certain numbers of surface or profiler data available. Here we consider another approach, restricting the solutions by some simple constraints.

A major characteristic of this GPS tomography's multiplicity is that certain increments at lower levels can be cancelled by some opposite increments at upper levels. However, in real atmosphere, the water vapor exponentially decays with height. Around 10 km height levels, water vapor is about 0.1 g/m^3 comparing to 10 g/m^3 near the ground. A rational increment at upper levels of the domain cannot be large enough to cancel increments at lower levels. If a water vapor analysis is constrained to small values near 10 km or above, large-scale vertical water vapor distribution could be determined uniquely. Another source of multiplicity could be mended if the water vapor is restricted to be non-negative. In this study we demonstrate the water vapor analysis using these simple constraints without other accurate water vapor observations, even though they may or may not be available in the IHOP region. To compare the analyses to satellite images, these constraints are found quite satisfactory.

4. GPS ANALYSIS

The tomography approach along with some simple constraints is applied to the dataset collected as a part of the International H2O Project (IHOP) 2002. At the right center of the IHOP region bounded by the left bottom corner at latitude and longitude (34.5, -100.0) and the upper right corner at (38.5, -95.0), there are 25 stations with GPS receivers. The network of stations is a combination of NOAA/FSL stations, SuomiNet stations, and special stations deployed by CNRS CNRM/GAME, France. The GPS data were processed using the Bernese 4.2 GPS

Software. Final satellite orbits from the International GPS Service (IGS) were used in the analysis and the station coordinates were constrained to their ITRF 2000 coordinates by incorporating GPS station data from IGS stations within the continental United States. The GPS data were processed using a double difference processing strategy to compute PW. Slant water values were computed in a similar manner as described by Braun et al., 2003.

During the IHOP 2002 (13 May-25 June 2002), there were storms over the right center of IHOP region on June 12 and 13, 2002. Over this time period, there were satellite water vapor images available at *http://www.joss.ucar.edu/ihop/dm/archive/.* These images can be used to qualitatively verify the water vapor distribution patterns of GPS slant tomography analysis. In this study, we choose an exponentially decaying function of height which has value of 10 gram/m^3 at the ground and 0.1 gram/m^3 at 10 km height. We penalize the difference between this function and the grid analysis at the top 4 levels of the grid. The vertical domain ranges from the ground up to 10 km. The analysis grid has 21 grid points in each direction. We solve the tomography problem under a simple bound, $w \geq 0$.

For a given analysis time, we collect all GPS data from these stations during a half hour interval which ranges from before 15 minutes to after 15 minutes of this given time. Treating all of these data as GPS observations at the given time, we increased the total number of GPS slant water vapor observations if the water vapor distribution does not change dramatically during this time period. This helps to determine large-scale water vapor distributions with the simple constraints.

For the given domain, we choose GPS slants whose ray paths are through the top of the domain and remove the others. With all of the GPS slants passing through the top domain, the minimum elevation angle used is about 7 degree, a little lower than the value, 10 degree, validated by Braun et al., 2003.

We presented here two analyses at 00:00 UTC, June 13, 2002 and 22:00 UTC, June 13, 2002. Since the integrated slant water vapor (integrated water vapor density along the ray path between a GPS satellite and a receiver, Bevis et al. 1992) is analyzed in this tomography, the unit of the analyzed water vapor is kg/m^3. To qualitatively verify the GPS tomography analysis, we compared them to the satellite water vapor images over the same area and found that they are highly correlated. Figures 4 and 5 show the contour plots of horizontal water vapor analyses at one km height comparing to satellite images of water vapor taken at the same time.

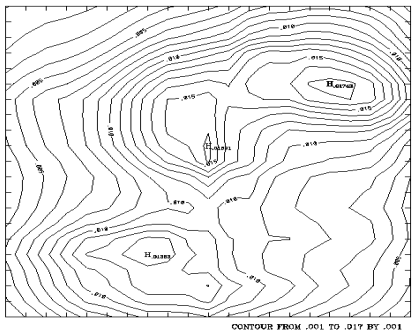

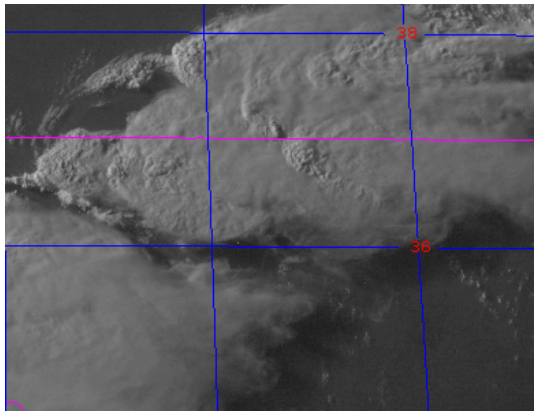

Fig. 4. *GPS tomography analysis at 00:00Z on June 13, 2002 (above) and a satellite image taken at the same time.*

Particularly on the stronger storm at 0:00 UTC, June 13, the analysis represents the storm very well, even showing the gap between two major high water vapor density blocks. Figure 6 shows the water vapor as height at the IHOP central facility. The red one is collected from a sounding, and the black one is the GPS slant tomography analysis. We believe that without certain accuracy of the GPS slant data and the tomography algorithm, we cannot obtain the analyses with such correlations to the satellite images.

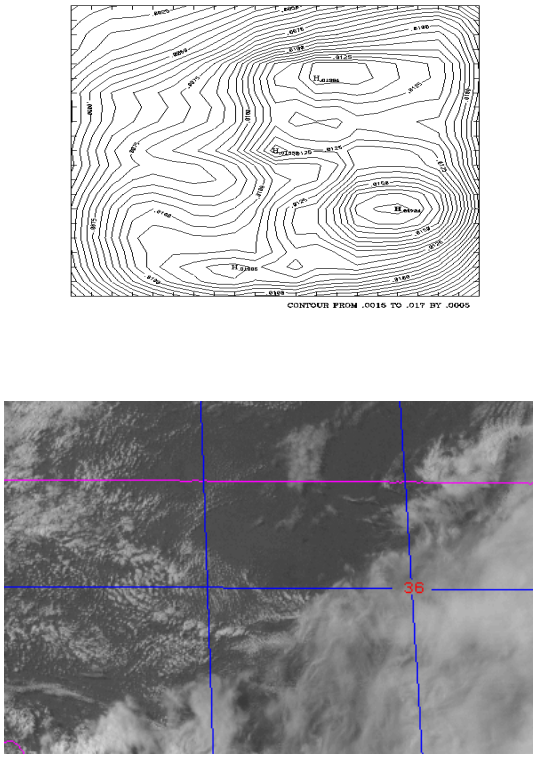

Fig. 5. *GPS tomography analysis at 22:00Z on June 13, 2002 (above) and a satellite image taken at the same time.*

5. CONCLUSIONS

Using processed slant water vapor (SW) from the right center of the IHOP domain, a GPS tomography technique provides water vapor analyses under simple water vapor constraints. Comparing to GOES satellite water vapor images and sounding data, these analyses resemble the basic storm feature during the time period of June 12 to 13, 2003. These analyses further confirm the conclusions made by MacDonald et al., (2002) under OSSE. These imply that the GPS tomography methods can extract useful information from GPS slants in real time GPS observations. These real-time experiments also confirm the quality of data processing from GPS slant water vapor delays into slant water vapor on these cases. For these cases, the data processing must have good accuracy; otherwise, we cannot obtain a reasonable storm pattern. We also ran these cases with shorter time intervals, i.e., with less slants, and found the analyses deteriorate as the amount of slant data decreases. To a certain degree, this shows that the slants, indeed, help the analyses.

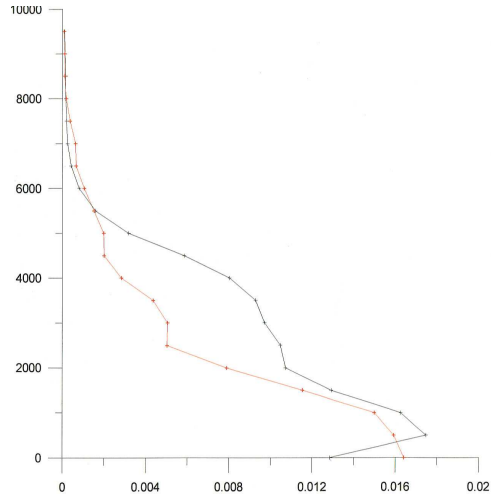

Fig. 6. *Vertical profiles of sounding and GPS tomography analysis at the central facility of IHOP region at 00:00Z on June 13, 2002.*

As GPS slants are removed, if they pass through the horizontal side boundaries of the domain of interest, there will be much less slants with low elevation angles near the boundaries in the tomography analysis. Thus, the analysis loses its accuracy near the horizontal boundaries, particularly at lower levels. This GPS network domain in this study is small, just 500 km by 500 km, and the boundary effect could damage the accuracy of the analysis in the center. For a large domain with the similar GPS receiver density, we can expect better results as more slants pass through the top of the domain and less boundary effect.

6. REFERENCES

Bevis, M., S. Businger, S. Chiswell, T. A. Herring, R. A. Anthes, C. Rocken, and R. Ware, 1994: Mapping zenith wet delays onto precipitable water. *J. Appl. Meteorol.*, **33**, 379-386.

Braun, J., C. Rocken, and R. Ware, 2001: Validation of line-of-sight water vapor measurements with GPS. *Radio Science*, **36**, 459-472.

Braun, J., C. Rocken, J. Liljegren, 2003: Comparisons of line-of-sight water vapor observations using the Global Positioning

System and a pointing microwave radiometer. *J. Atmos. Ocean. Tech*., **20**, 606-612.

Byrd, R. H., P. Lu, J. Nocedal, and C. Zhu, 1995: A limited memory algorithm for bound constrained optimization. *SIAM J. Scientific Computing*, **16**, no. 5.

Giering, R, and T. Kaminski, 1998: Recipes for adjoint code construction. *ACM Trans. On Math. Software*, **24**, No. 5, 437-474.

Hayden, C. M., and R. J. Purser, 1995: Recursive filter objective analysis of meteorological fields: Applications to NESDIS operational processing. *Journal of Appl. Meteor.*, **34**, 3-15.

MacDonald, A., Y. Xie, and R. Ware, 2002: Diagnosis of three dimensional water vapor using slant observations from a GPS network. *Mon. Wea. Rev.*, **130**, 386-397.

MacDonald, A., and Y. Xie, 2003: GPS surface station density requirements for recovery of three-dimensional water vapor. Invited Presentation, International Workshop on GPS Meteorology, Tsukuba, Japan.